ACS ENVIRONMENTAL Au
AN OPEN ACCESS JOURNAL OF THE AMERICAN CHEMICAL SOCIETY

pubs.acs.org/environau Article

Binding Between Antibiotics and Polystyrene Nanoparticles Examined by NMR

Saduni S. Arachchi, Stephanie P. Palma, Charlotte I. Sanders, Hui Xu, Rajshree Ghosh Biswas, Ronald Soong, André J. Simpson, and Leah B. Casabianca*

Cite This: *ACS Environ. Au* 2023, 3, 47–55 Read Online

ACCESS | Metrics & More | Article Recommendations

ABSTRACT: Elucidating the interactions between plastic nanoparticles and small molecules is important to understanding these interactions as they occur in polluted waterways. For example, plastic that breaks down into micro- and nanoscale particles will interact with small molecule pollutants that are also present in contaminated waters. Other components of natural water, such as dissolved organic matter, will also influence these interactions. Here we use a collection of complementary NMR techniques to examine the binding between polystyrene nanoparticles and three common antibiotics, belonging to a class of molecules that are expected to be common in polluted water. Through examination of proton NMR signal intensity, relaxation times, saturation-transfer difference (STD) NMR, and competition STD-NMR, we find that the antibiotics have binding strengths in the order amoxicillin < metronidazole ≪ levofloxacin. Levofloxacin is able to compete for binding sites, preventing the other two antibiotics from binding. The presence of tannic acid disrupts the binding between levofloxacin and the polystyrene nanoparticles, but does not influence the binding between metronidazole and these nanoparticles.

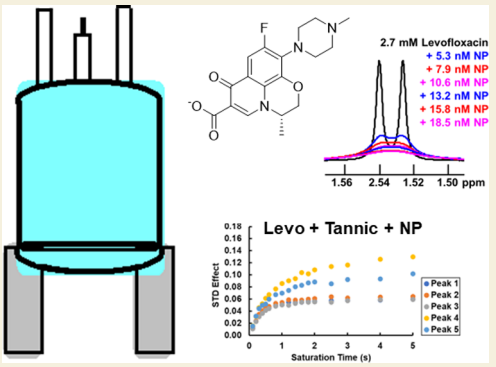

KEYWORDS: *antibiotics, NMR, polystyrene, nanoparticles, metronidazole, amoxicillin, levofloxacin*

INTRODUCTION

The amount of plastic pollution in world waterways is a growing concern.[1] The coronavirus pandemic has increased plastic waste through increased use and improper disposal of medical supplies and personal protective equipment (PPE), lifting of bans on single-use plastic bags, closing of recycling facilities, and increased demand for single-use plastic cutlery and plastic food packaging for restaurant take-out and delivery orders.[2] This plastic waste is especially dangerous to wildlife, who can become entangled in plastic or mistake it for food. Over time, large plastic pieces break down into micro- and nano-sized particles, and these small plastic particles pose hazards as well.[3,4] Fish that consume polystyrene nanoparticles have altered feeding behavior and metabolism.[5] Nanoparticles cross the blood-brain barrier to localize in the brain, changing the appearance of brain tissue and disrupting brain function.[5,6] The size of the nanoparticle influences the severity of the behavioral effects observed.[6] Nanoscale plastic in the ocean is also a concern to human health, as plastic nanoparticles have been shown to move up the food chain, from algae to zooplankton to fish.[6] Plastic particles have even been found in fish intended for human consumption.[7]

In addition to negative effects from the plastic particles themselves, nanoscale plastic can endanger aquatic life and human consumers of fish by concentrating toxic small molecules.[8] Harmful chemicals including endocrine disruptors such as bisphenol A (BPA), carcinogens including polycyclic aromatic hydrocarbons (PAHs), and pharmaceuticals, including antibiotics and anti-depressants, are taken up by plastic, and can leach out over time into organisms that consume these plastics.[9] Thus there is a pressing need to understand the mechanism of sorption (either absorption or adsorption) of small molecules into plastic micro- and nanoparticles.

Antibiotics are one class of common small molecule pollutants that are found along with plastic in polluted waterways, and could lead to health concerns including promoting the development of drug-resistant bacteria. Antibiotics also contain a variety of organic functional groups that are common to small molecules, including aromatic and non-aromatic rings, heteronuclei (including nitrogen and fluorine), stereocenters, and carboxylate groups. As such, they are excellent model compounds for demonstrating techniques that

Received: August 12, 2022
Revised: October 10, 2022
Accepted: October 12, 2022
Published: October 24, 2022

https://doi.org/10.1021/acsenvironau.2c00047
ACS Environ. Au 2023, 3, 47–55

aim to examine the binding between small molecules and plastic particles.

Dissolved organic matter (DOM) is also present in natural water, and influences the binding between small molecules and plastic particles. DOM consists of soluble organic matter that results from decomposition of plant and animal matter.[10] DOM is a heterogeneous mixture that contains humic and tannic acids, among other components. For example, Zhang et al.[11] observed that addition of humic acid decreased binding between fluoroquinolines (norfloxacin and levofloxacin) and either pristine or −COOH modified polystyrene nanoparticles. Interactions between fluoroquinolines and humic acid have been studied using a variety of techniques, including fluorescence quenching[12,13] and NMR spectroscopy.[13] Similar methods have been used to examine the binding between humic acid and halogenated phenols,[14] polycyclic aromatic hydrocarbons,[15] and polystyrene microparticles.[16] Humic acid and tannic acid are both major components of dissolved organic matter. However, humic acid is variable and the results will depend on the source of the humic acid and the amount of purification done on the sample. Thus, we have used tannic acid in our studies, as this compound is well-defined and has been used previously as a model for DOM.[17]

The saturation-transfer difference NMR (STD-NMR) experiment[18,19] is used to study small molecule ligands interacting with a large receptor particle. Two experiments are performed—an on-resonance experiment and an off-resonance or reference experiment. In the on-resonance experiment, the receptor is saturated with radio frequency irradiation for a given period of time. In the off-resonance experiment, saturation is performed for the same amount of time but at a frequency that is far from where the receptor and ligand resonances appear. When a small molecule ligand interacts with the receptor during the saturation time, part of the saturation is transferred from the receptor to the ligand, and the ligand NMR signal decreases in intensity. Ligands that do not interact with the receptor have the same signal intensity in the on-resonance and off-resonance spectra. Subtracting the on-resonance spectrum from the off-resonance spectrum therefore gives a difference spectrum containing only resonances from those ligands that interact with the receptor during the saturation time. The STD-NMR technique has the advantage that it can not only determine whether a particular ligand binds to a large receptor, but can also give insight into the binding geometry by identifying binding epitopes on the small molecule. Another advantage of using STD-NMR to study binding to nanoparticles is that the large receptor does not need to be seen by solution-state NMR, so there is no theoretical upper limit to the size of the receptor that can be studied.

Variations on the STD-NMR approach have also been useful in studying molecules interacting with DOM in natural waterways. Saturation-transfer double difference NMR (STDD-NMR) was used to determine the epitope map for pesticides with and without halogens interacting with humic acid.[20] A novel STD-NMR technique called reversed heteronuclear saturation transfer difference (RHSTD) NMR has been used to study the interactions between organofluorine contaminants and humic acid.[21−24] This technique can determine the components of humic acid that interact with the organofluorine by saturating the ^{19}F nuclei in the contaminant and transferring saturation to ^{1}H nuclei in the humic acid (receptor). The difference spectrum is then used to identify the components of humic acid that are responsible for binding to the organofluorine.

Many field[25−27] and laboratory[28−33] studies have been undertaken in order to quantify the amount and types of small molecule xenobiotics interacting with plastic in the environment, yet few studies are aimed at understanding the mechanism of sorption. However, NMR spectroscopy is a powerful technique for atomic-level structure determination, and has been extensively used to study small molecules interacting with nanoparticles in both the solid state[34−49] and solution state.[50−66] Different NMR experiments can provide complementary information about nanoparticle-small molecule binding, leading to an overall picture of the binding mechanism. This understanding is important in developing structure−activity relationships for binding between small molecules and large plastic particles. Understanding the properties of nanoparticles and small molecules that lead to increased sorption will be important to the design of plastic that minimizes sorption of toxic small molecules and the development of regulatory policy regarding the kinds and amounts of these toxic small molecules that are permitted in fish intended for human consumption.

METHODS

Amoxicillin, metronidazole, levofloxacin (analytical standard grade), and tannic acid (ACS reagent) were purchased from Sigma-Aldrich (St. Louis, MO) and were used without further purification. Carboxylate-modified (CML) polystyrene latex nanobeads (0.045 μm, 4 wt %) were purchased from Thermo Fisher Scientific (Waltham, MA). Deuterium oxide was purchased from Cambridge Isotope Labs (Tewksbury, MA). Deionized water was prepared using a Millipore Milli-Q purifier.

Samples were prepared in 100 mM phosphate buffer, pH 7, prepared in D_2O. The pH was read directly from the pH meter without any correction for isotope effects. A trace amount of trimethylsilyl propionate (TSP) was added to the buffer for chemical shift referencing. Samples were prepared by dissolving a known mass of antibiotic in phosphate-buffered D_2O, then adding the polystyrene nanoparticle suspension in H_2O. Control samples were prepared by adding the same volume of H_2O in place of the nanoparticle suspension.

Solution-state NMR measurements were made on a Bruker Avance NEO 500 MHz NMR spectrometer with Prodigy nitrogen-cooled cryoprobe or on a Bruker Avance NEO 500 MHz NMR with a Bruker SmartProbe. For quantitative one-dimensional proton spectra, the proton 90°-pulse length was carefully calibrated for each sample (ranging from 12.50−13.75 μs on the spectrometer with Prodigy cryoprobe and 8.50−8.88 μs on the spectrometer with SmartProbe), the spectral width was 11.76 and 15.62 ppm, and an acquisition time of 3.000 and 2.097 s was used for each spectrometer, respectively. In each case, 16 scans were collected after 4 dummy scans, and the free induction decay (FID) was zero-filled to 32,768 points before Fourier transform. A recycle delay of 12.5 s was used. This recycle delay is at least 5 times the measured T_1 relaxation time of each proton peak, with the exception of peak 3 of metronidazole. This peak was therefore not used for quantification.

STD experiments were performed using the standard Bruker pulse sequence "stddiffesgp",[18,19] where a train of 50 ms Gaussian pulses was used to achieve saturation. Off-resonance saturation was performed at 40 ppm and on-resonance saturation was performed at 12 ppm. The recycle delay was 7.0 s, and the saturation time ranged from 0.1 to 5.0 s in order to create the STD buildup curves. The on- and off-resonance spectra were collected in an interleaved manner. The STD experiment was acquired with a 1.500 or 2.097 s acquisition time, 32 or 64 scans, 4 dummy scans and 14.9 or 15.6 ppm spectral width. For both one-dimensional (1D) ^{1}H and STD experiments, the excitation sculpting with gradients water suppression sequence was

https://doi.org/10.1021/acsenvironau.2c00047
ACS Environ. Au 2023, 3, 47−55

used.[67] All experiments were done at 298.0 K. Bruker Topspin 4.0.6 software was used to process all NMR spectra. A custom-written MATLAB script was used to process phase-corrected spectra to calculate peak integrals. All MATLAB operations were done with MATLAB R2018a software (MathWorks, Natick, MA). The MATLAB scripts are available upon request from the corresponding author.

Proton spin-lattice relaxation times were measured using a standard inversion-recovery pulse sequence. Spin−spin relaxation times were measured using the "PROJECT" pulse sequence.[68] The spacing between pulses (τ) in the PROJECT sequence was 5 ms for the samples with polystyrene beads and 20 ms for the control samples. Excitation sculpting[67] was added at the end of the pulse sequence for water suppression.

RESULTS AND DISCUSSION

Figure 1 contains the one-dimensional proton NMR spectra of the antibiotics metronidazole, levofloxacin, and amoxicillin along with their proton peak assignments.

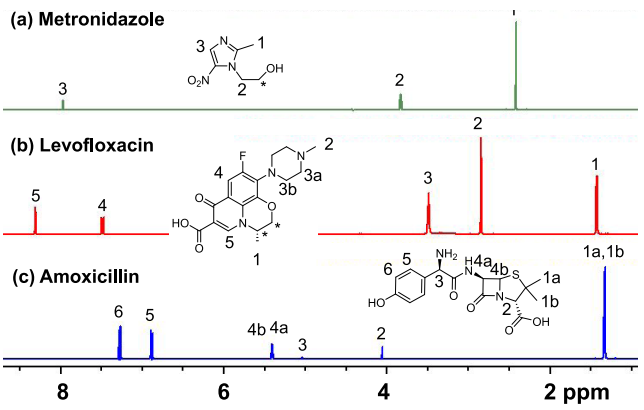

Figure 1. 1D ^{1}H NMR spectra and peak assignments for the three antibiotics considered in this study. Peak assignments were made with the assistance of refs 72, 73 and using two-dimensional NMR experiments (COSY, HSQC, and HMBC). * indicates protons that are not observed because their NMR signals appear within the region suppressed by the water suppression.

Upon addition of polystyrene nanoparticles, the NMR spectra of all antibiotics exhibit a decrease in signal intensity and an increase in line broadening, as shown in Figure 2. The decrease in signal intensity indicates strong binding, as molecules of antibiotic that bind strongly to the nanoparticle will exhibit rotational motion comparable to that of the large nanoparticle and become invisible in solution-state NMR. The fact that the levofloxacin signal decreases much more strongly with the addition of a smaller nanoparticle concentration than the other two antibiotics (see Figure 2d) indicates that there are many more binding sites on the nanoparticle for levofloxacin than for metronidazole and amoxicillin. Line broadening, on the other hand, indicates weak binding with an appreciable k_{off} rate constant so that the ligand is still observable in solution-state NMR. Line broadening is indicative of increased R_2 relaxation in the presence of the nanoparticle. When a solution-state molecule interacts weakly with a large receptor, the relaxation rate observed in solution will be a weighted average of the relaxation rate of the free and bound molecules. Since the relaxation of the bound state is expected to be significantly faster than that of the free state, the longer the molecule spends in the bound state, the shorter the observed T_2 relaxation time will be.[56,62]

The line broadening observed in Figure 2a−c prompted us to undertake a systematic study of the T_2 relaxation times of each sample. The measured R_2 relaxation rates ($R_2 = 1/T_2$) as a function of added nanoparticle concentration for each antibiotic are shown in Figure 3. The relaxivities (slope of the R_2*vs* concentration of nanoparticle added) are in the order levofloxacin ≫ metronidazole > amoxicillin which agrees with the decrease in signal intensity shown in Figure 2d. This indicates that levofloxacin interacts the most strongly with the polystyrene beads, as its relaxation times are the most influenced by the presence of the nanoparticles. The T_2 data for threonine, which has previously been shown not to bind significantly to the polystyrene beads, is shown in Figure 3d. This eliminates the possibility that there are paramagnetic impurities in the nanoparticles or other factors that are influencing the relaxation rates.

Saturation-Transfer Difference NMR

STD-NMR buildup curves for the different antibiotics interacting with the polystyrene nanoparticles are shown in Figure 4. For these STD experiments, we could not use the same antibiotic:nanoparticle ratio for each antibiotic. This is because the different antibiotics experience different amounts of line broadening at different nanoparticle concentrations. For example, if we added 264 nM nanoparticles to the levofloxacin sample, the levofloxacin signal would be broadened into the baseline and would not be observable. Conversely, adding only 5.3 nM nanoparticles to the amoxicillin sample would result in almost no observable interactions between the nanoparticles and amoxicillin. (See Figure 2) Thus, we chose antibiotic:nanoparticle ratios for each antibiotic such that the antibiotic signal intensity was about half that of the control sample. (These were the same samples used for the experiments shown in Figure 3). Since different ligand:receptor ratios were used, the STD effects were converted to STD amplification factors (STD_AF) for comparison. The amplification factor is found by multiplying the STD effect by the ligand:receptor ratio in order to normalize these effects, according to the following equations

$$\text{STD effect} = \frac{I}{I_0} \tag{1}$$

$$\text{STD\_AF} = \text{STD effect} \times \frac{[\text{L}]}{[\text{R}]} \tag{2}$$

Where I is the STD difference intensity, I_0 is the STD reference intensity, and [L] and [R] are the ligand and receptor concentrations, respectively.

The STD amplification factors for the three antibiotics are also in agreement with the signal intensity decrease and R_2 relaxivities, indicating that the binding strength is in the order levofloxacin ≫ metronidazole > amoxicillin. In all cases, the aromatic protons have a higher STD effect than other protons in the same molecule, indicating that the aromatic groups are responsible for binding.

Competition STD-NMR

In order to further verify this order of binding, we performed competition STD-NMR experiments. The results of these experiments are shown in Figure 5. The buildup curves for amoxicillin and metronidazole in the presence of polystyrene beads are shown in Figure 5a,d. Metronidazole protons exhibit higher STD effects than those of amoxicillin, indicating stronger binding. When amoxicillin and metronidazole are

https://doi.org/10.1021/acsenvironau.2c00047
ACS Environ. Au 2023, 3, 47−55

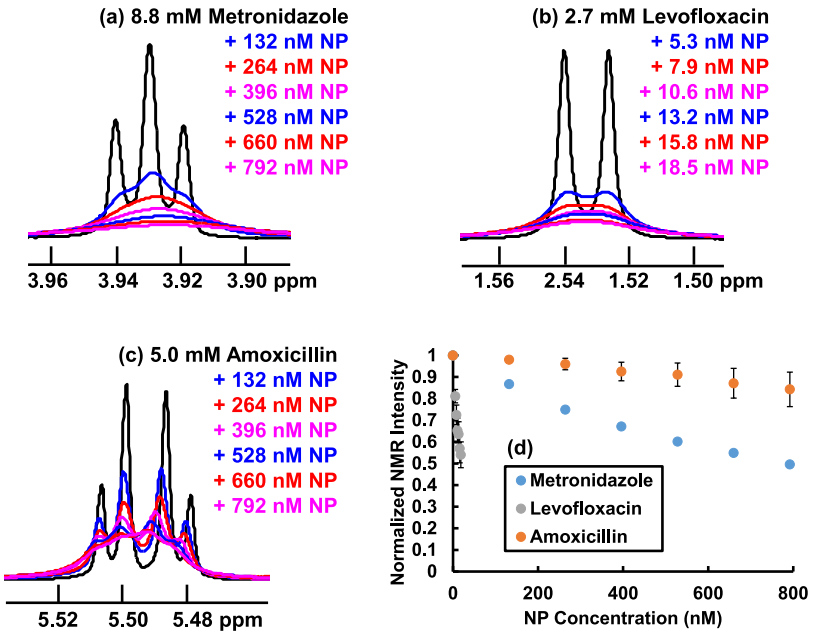

Figure 2. Line broadening and signal intensity decrease caused by the presence of polystyrene nanoparticles. (a–c) One or two representative NMR peaks for each antibiotic in the absence and presence of increasing concentrations of polystyrene nanoparticles (NP). (a) metronidazole, (b) levofloxacin, (c) amoxicillin. (d) Plot of normalized integral NMR intensity as a function of nanoparticle concentration for each antibiotic. Error bars represent standard deviation calculated over the individual NMR peaks. Peak 3 of metronidazole was not included in the intensity calculation due to the long T_1 relaxation time of this peak.

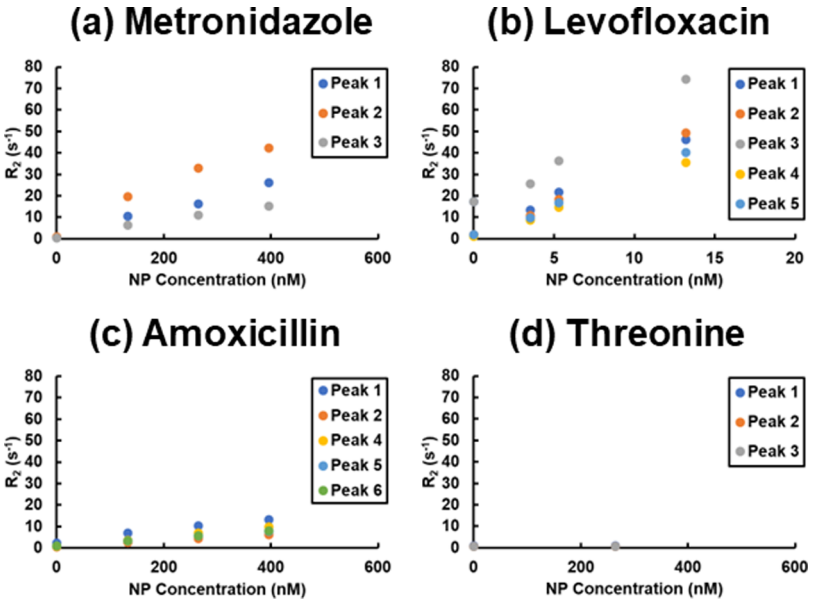

Figure 3. R_2 relaxation rates for (a) 9.2 mM metronidazole, (b) 3.0 mM levofloxacin, (c) 4.7 mM amoxicillin, and (d) 20.1 mM threonine in the presence of increasing concentrations of polystyrene nanoparticles. Threonine is included as a negative control. Note that the nanoparticle concentration in (b) is different from that in (a, c, d).

combined with polystyrene beads in the same sample, there is essentially no change in the STD buildup curves. However, when either metronidazole or amoxicillin is combined with levofloxacin in the presence of polystyrene beads, the STD effects of both amoxicillin and metronidazole decrease. Note that at this concentration of nanoparticles, all of the levofloxacin would be expected to be strongly bound according to Figure 2d, so no levofloxacin is observed in these spectra. These competition STD experiments suggest that levofloxacin binds more strongly than either metronidazole or amoxicillin, and is occupying binding sites on the polystyrene nanoparticle surface and preventing both metronidazole and amoxicillin from binding.

Previous studies have indicated that the binding between surface-modified polystyrene nanoparticles is related to the functional groups on the nanoparticles, with $\pi-\pi$ interactions, electrostatic interactions, and hydrophobic groups being important for binding.[51,53] However, the binding trends in the three antibiotics studied here do not lend themselves to a simple rationalization of the relative binding abilities. The

https://doi.org/10.1021/acsenvironau.2c00047
ACS Environ. Au 2023, 3, 47–55

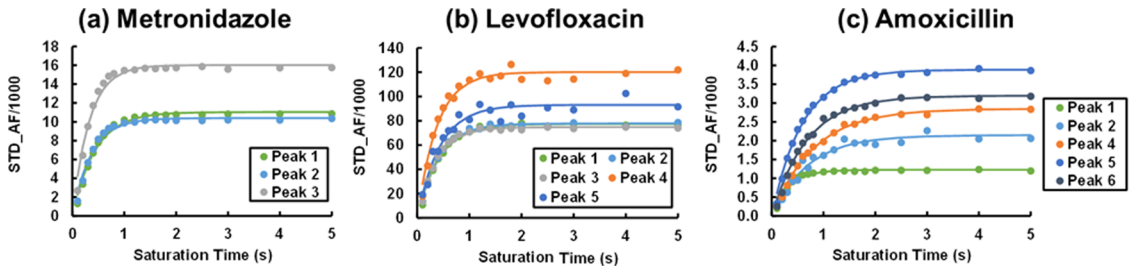

Figure 4. STD buildup curves for (a) 9.2 mM metronidazole in the presence of 264 nM polystyrene nanoparticles, (b) 3.0 mM levofloxacin in the presence of 5.3 nM polystyrene nanoparticles, and (c) 4.7 mM amoxicillin in the presence of 264 nM polystyrene nanoparticles.

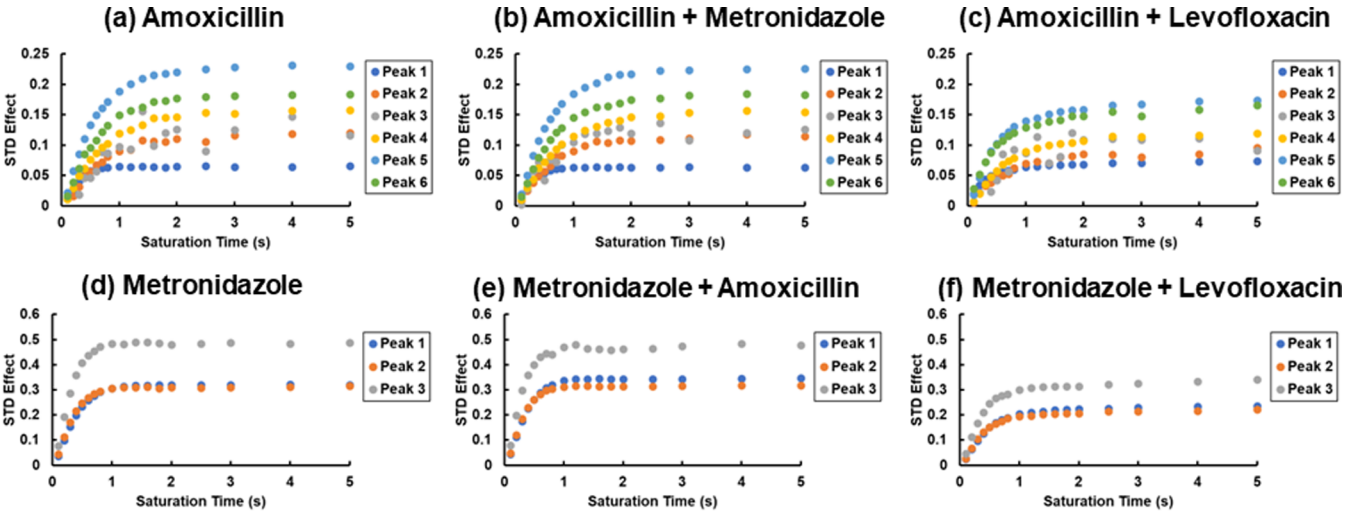

Figure 5. STD buildup curves for (a) 6 mM amoxicillin, (b) 6 mM amoxicillin in the presence of 9 mM metronidazole, (c) 6 mM amoxicillin in the presence of 9 mM levofloxacin, (d) 10 mM metronidazole (e) 9 mM metronidazole in the presence of 6 mM amoxicillin, (f) 10 mM metronidazole in the presence of 10 mM levofloxacin. Each sample also contained 0.8 wt % (264 nM) 40 nm polystyrene beads. Peak labels correspond to those in Figure 1.

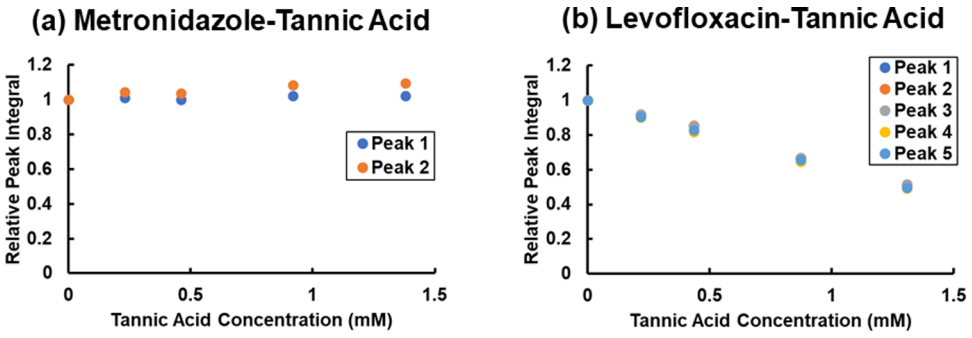

Figure 6. Normalized NMR signal intensity for (a) 11.0 mM metronidazole and (b) 12.7 mM levofloxacin in the presence of increasing concentrations of tannic acid.

antibiotics are complicated molecules, with levofloxacin and amoxicillin both having aromatic and carboxylate groups and metronidazole having aromatic, −OH, and nitro groups, among others. Interestingly, levofloxacin, which was found to have the largest number of binding sites per nanoparticle, is the only one of the three that should have an overall negative charge[69,70] at pH 7. This should lead to unfavorable interactions between levofloxacin and the negatively-charged polystyrene surface. These results indicate that the binding between surface-modified polystyrene nanoparticles and small molecules is more complicated than previously thought. However, levofloxacin does contain a fluorine group, which is strongly hydrophobic. The fluorine group has previously been shown to be responsible for binding between fluorine-containing xenobiotics and hydrophobic natural organic matter.[22] The presence of fluorine in levofloxacin could therefore explain the unexpected strong propensity for levofloxacin to bind to these nanoparticles, and indicates that hydrophobic effects can be the dominant factor for this kind of binding in the case of very hydrophobic groups on the small molecule.

Presence of Dissolved Organic Matter

When considering plastic particles interacting with small molecules in natural waterways, it is also important to consider other components of these waters. Here we explore how the

https://doi.org/10.1021/acsenvironau.2c00047
ACS Environ. Au 2023, 3, 47−55

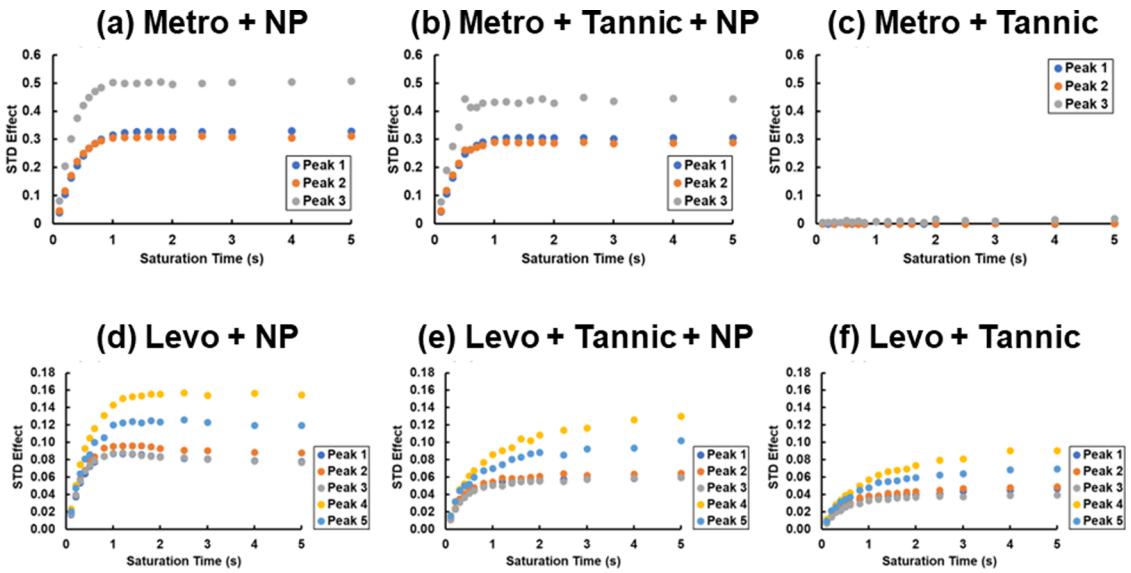

Figure 7. STD buildup curves for metronidazole (metro) and levofloxacin (levo) in the presence of either polystyrene nanoparticles, tannic acid, or both. (a) 9.8 mM metronidazole and 260 nM nanoparticles, (b) 9.8 mM metronidazole, 260 nM nanoparticles, and 0.843 mM tannic acid, (c) 9.8 mM metronidazole and 0.823 mM tannic acid, (d) 13.2 mM levofloxacin and 26 nM nanoparticles, (e) 13.2 mM levofloxacin, 26 nM nanoparticles, and 0.823 mM tannic acid, (f) 13.2 mM levofloxacin and 0.823 mM tannic acid.

presence of tannic acid influences the binding of metronidazole and levofloxacin with polystyrene nanoparticles.

First, Figure 6 shows the NMR signal intensity of metronidazole and levofloxacin in the presence of increasing amounts of tannic acid. Some decomposition was observed for amoxicillin at room temperature during the time required for these experiments, so amoxicillin was not considered here. Whereas the presence of up to 1.5 mM tannic acid does not influence the signal intensity of metronidazole, the signal intensity of levofloxacin decreases with addition of tannic acid. Notably, visible precipitation was observed in the levofloxacin-tannic acid samples as well.

In Figure 7, we examine the binding between the two antibiotics and polystyrene nanoparticles in the presence of tannic acid using STD-NMR. Figure 7a–c show the STD buildup curves for samples containing metronidazole and nanoparticles; metronidazole, nanoparticles, and tannic acid; and metronidazole and tannic acid, respectively. When tannic acid is added to a sample containing metronidazole and nanoparticles, the STD buildup curve of the metronidazole is only slightly affected, as can be seen by comparing Figure 7a,b. The initial slope of the STD buildup curve does not change significantly ($1.55 \pm 0.05\ s^{-1}$ without tannic acid, Figure 7a to $1.50 \pm 0.08\ s^{-1}$ with tannic acid, Figure 7b) Additionally, no STD effect is observed for metronidazole in the presence of tannic acid only, without nanoparticles. This indicates that tannic acid is not disturbing the binding between metronidazole and nanoparticles, and is in agreement with tannic acid not having strong interactions with metronidazole as was observed in Figure 6a.

When tannic acid is added to a sample containing levofloxacin and nanoparticles, however, a decrease in the STD effect, as well as a decrease in the initial slope of the STD buildup curve, is observed for all peaks. The initial slope of the STD buildup curve is often used as a measure of the relative strength of interaction, since it is less sensitive to the effects of relaxation and ligand re-binding than individual STD effects measured at longer saturation times.[71] A decrease in the initial slope indicates that the binding is actually being affected, rather than the STD buildup curve being influenced by the presence of paramagnetic impurities or other effects that would only decrease the T_1 relaxation times. Notably, there is also an observable STD effect for levofloxacin in the presence of tannic acid only, even without the addition of polystyrene nanoparticles. In the sample containing levofloxacin, nanoparticles, and tannic acid (Figure 7e), levofloxacin binds to both the polystyrene nanoparticles and tannic acid, so that the STD buildup curve is between the two.

CONCLUSIONS

We have used several complementary NMR techniques to examine the binding between polystyrene nanoparticles and common antibiotics that may be present in polluted waterways. Based on measurements of NMR signal intensity, relaxation rates, STD amplification factors, and competition STD-NMR experiments, we can conclude that the binding strength between the three antibiotics and polystyrene nanoparticles increases in the order amoxicillin < metronidazole ≪ levofloxacin. This is consistent with levofloxacin having a fluorine group, which is hydrophobic and has been shown previously to be a functional group that is responsible for binding in a hydrophobic environment.[22] Tannic acid, a component of dissolved organic matter that is also expected to be present in polluted waterways, was shown to influence the binding between levofloxacin and polystyrene nanoparticles but not the binding between metronidazole and nanoparticles.

This work provides valuable information about the binding between three common antibiotics and surface-modified polystyrene nanoparticles. Understanding the interactions between nanoscale plastics and xenobiotics that may be present in polluted waterways, as well as how dissolved organic matter influences these interactions, will be useful in designing remediation strategies.

https://doi.org/10.1021/acsenvironau.2c00047
ACS Environ. Au 2023, 3, 47–55

AUTHOR INFORMATION

Corresponding Author

Leah B. Casabianca − *Department of Chemistry, Clemson University, Clemson, South Carolina 29634, United States;* orcid.org/0000-0001-9447-3236; Email: lcasabi@clemson.edu

Authors

Saduni S. Arachchi − *Department of Chemistry, Clemson University, Clemson, South Carolina 29634, United States*

Stephanie P. Palma − *Department of Chemistry, Clemson University, Clemson, South Carolina 29634, United States*

Charlotte I. Sanders − *Department of Chemistry, Clemson University, Clemson, South Carolina 29634, United States*

Hui Xu − *Department of Chemistry, Clemson University, Clemson, South Carolina 29634, United States*

Rajshree Ghosh Biswas − *Department of Chemistry, University of Toronto Scarborough, Toronto, Ontario M1C 1A4, Canada*

Ronald Soong − *Department of Chemistry, University of Toronto Scarborough, Toronto, Ontario M1C 1A4, Canada;* orcid.org/0000-0002-8223-9028

André J. Simpson − *Department of Chemistry, University of Toronto Scarborough, Toronto, Ontario M1C 1A4, Canada;* orcid.org/0000-0002-8247-5450

Complete contact information is available at: https://pubs.acs.org/10.1021/acsenvironau.2c00047

Author Contributions

CRediT: **Saduni S. Arachchi** conceptualization (lead), investigation (equal), writing-review & editing (equal); **Stephanie P. Palma** investigation (equal), writing-review & editing (equal); **Charlotte I. Sanders** investigation (equal), writing-review & editing (equal); **Hui Xu** investigation (equal), supervision (equal), writing-review & editing (equal); **Rajshree Ghosh Biswas** formal analysis (equal), writing-review & editing (equal); **Ronald Soong** formal analysis (equal), writing-review & editing (equal); **André J. Simpson** formal analysis (equal), supervision (equal), validation (equal), writing-review & editing (equal); **Leah Beck Casabianca** conceptualization (supporting), data curation (equal), formal analysis (equal), funding acquisition (equal), investigation (equal), methodology (equal), project administration (lead), resources (equal), supervision (equal), validation (equal), visualization (equal), writing-original draft (lead), writing-review & editing (equal).

Notes

The authors declare no competing financial interest.

ACKNOWLEDGMENTS

We thank the NSF (CHE-1751529 and CHE-1725919) for support of this research. CIS was supported by an NSF REU grant (CHE-2050042). Thanks also go to an anonymous reviewer of one of our proposals for suggesting the work with dissolved organic matter.

REFERENCES

(1) Jambeck, J. R.; Geyer, R.; Wilcox, C.; Siegler, T. R.; Perryman, M.; Andrady, A.; Narayan, R.; Law, K. L. Plastic waste inputs from land into the ocean. *Science* **2015**, *347*, 768−771.

(2) Prata, J. C.; Silva, A. L. P.; Walker, T. R.; Duarte, A. C.; Rocha-Santos, T. COVID-19 Pandemic Repercussions on the Use and Management of Plastics. *Environ. Sci. Technol.* **2020**, *54*, 7760−7765.

(3) Andrady, A. L. The Plastic in Microplastics: A Review. *Mar. Pollut. Bull.* **2017**, *119*, 12−22.

(4) Andrady, A. L. Microplastics in the Marine Environment. *Mar. Pollut. Bull.* **2011**, *62*, 1596−1605.

(5) Mattsson, K.; Ekvall, M. T.; Hansson, L.-A.; Linse, S.; Malmendal, A.; Cedervall, T. Altered Behavior, Physiology, and Metabolism in Fish Exposed to Polystyrene Nanoparticles. *Environ. Sci. Technol.* **2015**, *49*, 553−561.

(6) Mattsson, K.; Johnson, E. V.; Malmendal, A.; Linse, S.; Hansson, L.-A.; Cedervall, T. Brain damage and behavioural disorders in fish induced by plastic nanoparticles delivered through the food chain. *Sci. Rep.* **2017**, *7*, No. 11452.

(7) Rochman, C. M.; Tahir, A.; Williams, S. L.; Baxa, D. V.; Lam, R.; Miller, J. T.; Teh, F.-C.; Werorilangi, S.; Teh, S. J. Anthropogenic Debris in Seafood: Plastic Debris and Fibers From Textiles in Fish and Bivalves Sold for Human Consumption. *Sci. Rep.* **2015**, *5*, No. 14340.

(8) Rochman, C. M.; Hoh, E.; Kurobe, T.; Teh, S. J. Ingested plastic transfers hazardous chemicals to fish and induces hepatic stress. *Sci. Rep.* **2013**, *3*, No. 3263.

(9) Fred-Ahmadu, O. H.; Bhagwat, G.; Oluyoye, I.; Benson, N. U.; Ayejuyo, O. O.; Palanisami, T. Interaction of chemical contaminants with microplastics: Principles and perspectives. *Sci. Total. Environ.* **2000**, *706*, No. 135978.

(10) https://www.usgs.gov/labs/organic-matter-research-laboratory/what-organic-matter-0. (Accessed August 11, 2022)

(11) Zhang, H.; Liu, F.-f.; Wang, S.-c.; Huang, T.-y.; Li, M.-r.; Zhu, Z.-l.; Liu, G.-z. Sorption of fluoroquinolones to nanoplastics as affected by surface functionalization and solution chemistry. *Environ. Pollut.* **2020**, *262*, No. 114347.

(12) Ferrie, R. P.; Hewitt, G. E.; Anderson, B. D. A Fluorescence Quenching Analysis of the Binding of Fluoroquinolones to Humic Acid. *Appl. Spectrosc.* **2017**, *71*, 2512−2518.

(13) Zhao, X.; Hu, Z.; Yang, X.; Cai, X.; Wang, Z.; Xie, X. Noncovalent interactions between fluoroquinolone antibiotics with dissolved organic matter: A ^{1}H NMR binding site study and multi-spectroscopic methods. *Environ. Pollut.* **2019**, *248*, 815−822.

(14) Šmejkalová, D.; Spaccini, R.; Fontaine, B.; Piccolo, A. Binding of Phenol and Differently Halogenated Phenols to Dissolved Humic Matter As Measured by NMR Spectroscopy. *Environ. Sci. Technol.* **2009**, *43*, 5377−5382.

(15) Simpson, M. J.; Simpson, A. J.; Hatcher, P. G. Noncovalent interactions between aromatic compounds and dissolved humic acid examined by nuclear magnetic resonance spectroscopy. *Environ. Toxicol. Chem.* **2004**, *23*, 355−362.

(16) Chen, W.; Ouyang, Z.-Y.; Qian, C.; Yu, H.-Q. Induced structural changes of humic acid by exposure of polystyrene microplastics: A spectroscopic insight. *Environ. Pollut.* **2018**, *233*, 1−7.

(17) Wu, L.; Dai, J.; Bi, E. Roles of dissolved humic acid and tannic acid in sorption of benzotriazole to a sandy loam soil. *Ecotoxicol. Environ. Saf.* **2020**, *204*, No. 111088.

(18) Mayer, M.; Meyer, B. Characterization of Ligand Binding by Saturation Transfer Difference NMR Spectroscopy. *Angew. Chem., Int. Ed.* **1999**, *38*, 1784−1788.

(19) Mayer, M.; Meyer, B. Group Epitope Mapping by Saturation Transfer Difference NMR To Identify Segments of a Ligand in Direct Contact with a Protein Receptor. *J. Am. Chem. Soc.* **2001**, *123*, 6108−6117.

(20) Shirzadi, A.; Simpson, M. J.; Xu, Y.; Simpson, A. J. Application of Saturation Transfer Double Difference NMR to Elucidate the Mechanistic Interactions of Pesticides with Humic Acid. *Environ. Sci. Technol.* **2008**, *42*, 1084−1090.

(21) Longstaffe, J. G.; Courtier-Murias, D.; Simpson, A. J. A nuclear magnetic resonance study of the dynamics of organofluorine

interactions with a dissolved humic acid. *Chemosphere* **2016**, *145*, 307−313.
(22) Longstaffe, J. G.; Simpson, A. J. Understanding solution-state noncovalent interactions between xenobiotics and natural organic matter using $^{19}F/^{1}H$ heteronuclear saturation transfer difference nuclear magnetic resonance spectroscopy. *Environ. Toxicol. Chem.* **2011**, *30*, 1745−1753.
(23) Longstaffe, J. G.; Simpson, M. J.; Maas, W.; Simpson, A. J. Identifying Components in Dissolved Humic Acid That Bind Organofluorine Contaminants using $^{1}H\{^{19}F\}$ Reverse Heteronuclear Saturation Transfer Difference NMR Spectroscopy. *Environ. Sci. Technol.* **2010**, *44*, 5476−5482.
(24) Longstaffe, J. G.; Courtier-Murias, D.; Simpson, A. J. The pH-dependence of organofluorine binding domain preference in dissolved humic acid. *Chemosphere* **2013**, *90*, 270−275.
(25) Rochman, C. M.; Manzano, C.; Hentschel, B. T.; Simonich, S. L. M.; Hoh, E. Polystyrene plastic: a source and sink for polycyclic aromatic hydrocarbons in the marine environment. *Environ. Sci. Technol.* **2013**, *47*, 13976−13984.
(26) Rochman, C. M.; Hoh, E.; Hentschel, B. T.; Kaye, S. Long-term field measurement of sorption of organic contaminants to five types of plastic pellets: implications for plastic marine debris. *Environ. Sci. Technol.* **2013**, *47*, 1646−1654.
(27) Van, A.; Rochman, C. M.; Flores, E. M.; Hill, K. L.; Vargas, E.; Vargas, S. A.; Hoh, E. Persistent organic pollutants in plastic marine debris found on beaches in San Diego, California. *Chemosphere* **2012**, *86*, 258−263.
(28) Wang, J.; Liu, X.; Liu, G. Sorption behaviors of phenanthrene, nitrobenzene, and naphthalene on mesoplastics and microplastics. *Environ. Sci. Pollut. Res.* **2019**, *26*, 12563−12573.
(29) Wang, W.; Wang, J. Comparative evaluation of sorption kinetics and isotherms of pyrene onto microplastics. *Chemosphere* **2018**, *193*, 567−573.
(30) Wang, W.; Wang, J. Different partition of polycyclic aromatic hydrocarbon on environmental particulates in freshwater: Microplastics in comparison to natural sediment. *Ecotoxicol. Environ. Saf.* **2018**, *147*, 648−655.
(31) Zhang, J.; Chen, H.; He, H.; Cheng, X.; Ma, T.; Hu, J.; Yang, S.; Li, S.; Zhang, L. Adsorption behavior and mechanism of 9-Nitroanthracene on typical microplastics in aqueous solutions. *Chemosphere* **2020**, *245*, No. 125628.
(32) Liu, G.; Zhu, Z.; Yang, Y.; Sun, Y.; Yu, D.; Ma, J. Sorption behavior and mechanism of hydrophilic organic chemicals to virgin and aged microplastics in freshwater and seawater. *Environ. Pollut.* **2019**, *246*, 26−33.
(33) Zuo, L.-Z.; Li, H.-X.; Lin, L.; Sun, Y.-X.; Diao, Z.-H.; Liu, S.; Zhang, Z.-Y.; Xu, X.-R. Sorption and desorption of phenanthrene on biodegradablepoly(butylene adipate co-terephtalate) microplastics. *Chemosphere* **2019**, *215*, 25−32.
(34) Chen, Y. H.; Dorn, R. W.; Hanrahan, M. P.; Wei, L.; Blome-Fernandez, R.; Medina-Gonzalez, A. M.; Adamson, M. A. S.; Flintgruber, A. H.; Vela, J.; Rossini, A. J. Revealing the Surface Structure of CdSe Nanocrystals by Dynamic Nuclear Polarization-Enhanced Se-77 and Cd-113 Solid-State NMR Spectroscopy. *J. Am. Chem. Soc.* **2021**, *143*, 8747−8760.
(35) Guo, C.; Jordan, J. S.; Yarger, J. L.; Holland, G. P. Highly Efficient Fumed Silica Nanoparticles for Peptide Bond Formation: Converting Alanine to Alanine Anhydride. *ACS Appl. Mater. Interfaces* **2017**, *9*, 17653−17661.
(36) Guo, C.; Holland, G. P. Alanine Adsorption and Thermal Condensation at the Interface of Fumed Silica Nanoparticles: A Solid-State NMR Investigation. *J. Phys. Chem. C* **2015**, *119*, 25663−25672.
(37) Guo, C.; Holland, G. P. Investigating Lysine Adsorption on Fumed Silica Nanoparticles. *J. Phys. Chem. C* **2014**, *118*, 25792−25801.
(38) Guo, C. C.; Holland, G. P.; Yarger, J. L. Lysine-Capped Silica Nanoparticles: A Solid-State NMR Spectroscopy Study. *MRS Adv.* **2016**, *1*, 2261−2266.
(39) Hanrahan, M. P.; Chen, Y.; Blome-Fernández, R.; Stein, J. L.; Pach, G. F.; Adamson, M. A. S.; Neale, N. R.; Cossairt, B. M.; Vela, J.; Rossini, A. J. Probing the Surface Structure of Semiconductor Nanoparticles by DNP SENS with Dielectric Support Materials. *J. Am. Chem. Soc.* **2019**, *141*, 15532−15546.
(40) Kumar, A.; Durand, H.; Zeno, E.; Balsollier, C.; Watbled, B.; Sillard, C.; Fort, S.; Baussane, I.; Belgacem, N.; Lee, D.; Hediger, S.; Demeunynck, M.; Bras, J.; De Paëpe, G. The surface chemistry of a nanocellulose drug carrier unravelled by MAS-DNP. *Chem. Sci.* **2020**, *11*, 3868−3877.
(41) Lee, D.; Kaushik, M.; Coustel, R.; Chenavier, Y.; Chanal, M.; Bardet, M.; Dubois, L.; Okuno, H.; Rochat, N.; Duclairoir, F.; Mouesca, J.-M.; De Paepe, G. Solid-State NMR and DFT Combined for the Surface Study of Functionalized Silicon Nanoparticles. *Chem. - Eur. J.* **2015**, *21*, 16047−16058.
(42) Lee, D.; Monin, G.; Doung, N. T.; Lopez, I. Z.; Bardet, M.; Mareau, V.; Gonon, L.; De Paepe, G. Untangling the Condensation Network of Organosiloxanes on Nanoparticles using 2D Si-29-Si-29 Solid-State NMR Enhanced by Dynamic Nuclear Polarization. *J. Am. Chem. Soc.* **2014**, *136*, 13781−13788.
(43) Lee, D.; Wolska-Pietkiewicz, M.; Badoni, S.; Grala, A.; Lewiński, J.; De Paëpe, G. Disclosing Interfaces of ZnO Nanocrystals Using Dynamic Nuclear Polarization: Sol-Gel versus Organometallic Approach. *Angew. Chem., Int. Ed.* **2019**, *58*, 17163−17168.
(44) Lee, D.; Leroy, C.; Crevant, C.; Bonhomme-Coury, L.; Babonneau, F.; Laruencin, D.; Bonhomme, C.; De Paëpe, G. Interfacial Ca^{2+} environments in nanocrystalline apatites revealed by dynamic nuclear polarization enhanced ^{43}Ca NMR spectroscopy. *Nat. Commun.* **2017**, *8*, No. 14104.
(45) Lee, D.; Duong, N. T.; Lafon, O.; De Paëpe, G. Primostrato Solid-State NMR Enhanced by Dynamic Nuclear Polarization: Pentacoordinated Al^{3+} Ions Are Only Located at the Surface of Hydrated γ-Alumina. *J. Phys. Chem. C* **2014**, *118*, 2565−2576.
(46) Roth, A. N.; Chen, Y. H.; Adamson, M. A. S.; Gi, E.; Wagner, M.; Rossini, A. J.; Vela, J. Alkaline-Earth Chalcogenide Nanocrystals: Solution-Phase Synthesis, Surface Chemistry, and Stability. *ACS Nano* **2022**, *16*, 12024−12035.
(47) Terlecki, M.; Badoni, S.; Leszczyński, M. K.; Gierlotka, S.; Justyniak, I.; Okuno, H.; Wolska-Pietkiewicz, M.; Lee, D.; De Paëpe, G.; Lewiński, J. ZnO Nanoplatelets with Controlled Thickness: Atomic Insight into Facet-Specific Bimodal Ligand Binding Using DNP NMR. *Adv. Funct. Mater.* **2021**, *31*, No. 2105318.
(48) Swanson, H. L.; Guo, C.; Cao, M.; Addison, J. B.; Holland, G. P. Probing the binding modes and dynamics of histidine on fumed silica surfaces by solid-state NMR. *Phys. Chem. Chem. Phys.* **2020**, *22*, 20349−20361.
(49) Casabianca, L. B. Solid-state nuclear magnetic resonance studies of nanoparticles. *Solid State Nucl. Magn. Reson.* **2020**, *107*, No. 101664.
(50) Zhang, Y.; Xu, H.; Parsons, A. M.; Casabianca, L. B. Examining Binding to Nanoparticle Surfaces Using Saturation Transfer Difference (STD)-NMR Spectroscopy. *J. Phys. Chem. C* **2017**, *121*, 24678−24686.
(51) Zhang, Y.; Casabianca, L. B. Probing Amino Acid Interaction with a Polystyrene Nanoparticle Surface Using Saturation-Transfer Difference (STD)-NMR. *J. Phys. Chem. Lett.* **2018**, *9*, 6921−6925.
(52) Zhang, Y.; Xu, H.; Casabianca, L. B. Interaction Between Cyanine Dye IR-783 and Polystyrene Nanoparticles in Solution. *Magn. Reson. Chem.* **2018**, *56*, 1054−1060.
(53) Xu, H.; Casabianca, L. B. Probing Driving Forces for Binding Between Nanoparticles and Amino Acids by Saturation-Transfer Difference NMR. *Sci. Rep.* **2020**, *10*, No. 12351.
(54) Xu, H.; Lustig, D.; Casabianca, L. B. ^{13}C Saturation-Transfer Difference (STD)-NMR Experiments Using INEPT Polarization Transfer. *Appl. Magn. Reson.* **2020**, *51*, 277−286.
(55) Xu, H.; Casabianca, L. B. A Dual Fluorescence and NMR Study for the Interaction Between Xanthene Dyes and Nanoparticles. *Langmuir* **2021**, *37*, 385−390.

https://doi.org/10.1021/acsenvironau.2c00047
ACS Environ. Au 2023, 3, 47−55

(56) An, Y.; Sedinkin, S. L.; Venditti, V. Solution NMR methods for structural and thermodynamic investigation of nanoparticle adsorption equilibria. *Nanoscale Adv.* **2022**, *4*, 2583−2607.
(57) Xiang, X. Y.; Hansen, A. L.; Yu, L.; Jameson, G.; Bruschweiler-Li, L.; Yuan, C. H.; Bruschweiler, R. Observation of Sub-Microsecond Protein Methyl-Side Chain Dynamics by Nanoparticle-Assisted NMR Spin Relaxation. *J. Am. Chem. Soc.* **2021**, *143*, 13593−13604.
(58) Xu, J. X.; Alom, M. S.; Fitzkee, N. C. Quantitative Measurement of Multiprotein Nanoparticle Interactions Using NMR Spectroscopy. *Anal. Chem.* **2021**, *93*, 11982−11990.
(59) Xue, M. J.; Sampath, J.; Gebhart, R. N.; Haugen, H. J.; Lyngstadaas, S. P.; Pfaendtner, J.; Drobney, G. Studies of Dynamic Binding of Amino Acids to TiO2 Nanoparticle Surfaces by Solution NMR and Molecular Dynamics Simulations. *Langmuir* **2020**, *36*, 10341−10350.
(60) Assfalg, M.; Ragona, L.; Pagano, K.; D'Onofrio, M.; Zanzoni, S.; Tomaselli, S.; Molinari, H. The study of transient protein-nanoparticle interactions by solution NMR spectroscopy. *Biochim. Biophys. Acta, Proteins Proteomics* **2016**, *1864*, 102−114.
(61) Wardenfelt, S.; Xiang, X. Y.; Xie, M. Z.; Yu, L.; Bruschweiler-Li, L.; Bruschweiler, R. Broadband Dynamics of Ubiquitin by Anionic and Cationic Nanoparticle Assisted NMR Spin Relaxation. *Angew. Chem., Int. Ed.* **2021**, *60*, 148−152.
(62) Perera, Y. R.; Hill, R. A.; Fitzkee, N. C. Protein Interactions with Nanoparticle Surfaces: Highlighting Solution NMR Techniques. *Isr. J. Chem.* **2019**, *59*, 962−979.
(63) Xie, M. Z.; Yu, L.; Bruschweiler-Li, L.; Xiang, X. Y.; Hansen, A. L.; Bruschweiler, R. Functional protein dynamics on uncharted time scales detected by nanoparticle-assisted NMR spin relaxation. *Sci. Adv.* **2019**, *5*, No. eaax5560.
(64) Sedinkin, S. L.; An, Y.; Naik, P.; Slowing, I. I.; Venditti, V. An organogel library for solution NMR analysis of nanoparticle suspensions in non-aqueous samples. *J. Magn. Reson.* **2020**, *321*, No. 106874.
(65) Egner, T. K.; Naik, P.; Nelson, N. C.; Slowing, I. I.; Venditti, V. Mechanistic Insight into Nanoparticle Surface Adsorption by Solution NMR Spectroscopy in an Aqueous Gel. *Angew. Chem., Int. Ed.* **2017**, *56*, 9802−9806.
(66) Egner, T. K.; Naik, P.; An, Y.; Venkatesh, A.; Rossini, A. J.; Slowing, I. I.; Venditti, V. 'Surface Contrast' NMR Reveals Non-innocent Role of Support in Pd/CeO(2)Catalyzed Phenol Hydrogenation. *ChemCatChem* **2020**, *12*, 4160−4166.
(67) Hwang, T. L.; Shaka, A. J. Water Suppression That Works. Excitation Sculpting Using Arbitrary Wave-Forms and Pulsed-Field Gradients. *J. Magn. Reson., Ser. A* **1995**, *112*, 275−279.
(68) Aguilar, J. A.; Nilsson, M.; Bodenhausen, G.; Morris, G. A. Spin echo NMR spectra without J modulation. *Chem. Commun.* **2012**, *48*, 811−813.
(69) Tsuji, A.; Nakashima, E.; Hamano, S.; Yamana, T. Physicochemical properties of amphoteric β-lactam antibiotics, I: stability, solubility, and dissolution behavior of amino penicillins as a function of pH. *J. Pharm. Sci.* **1978**, *67*, 1059−1066.
(70) http://www.drugbank.ca/drugs/DB00916, http://www.drugbank.ca/drugs/DB01137. (Accessed December 2020).
(71) Angulo, J.; Nieto, P. M. STD-NMR: application to transient interactions between biomolecules—a quantitative approach. *Eur. Biophys. J.* **2011**, *40*, 1357−1369.
(72) Baranova, A.; Huang, B. T.; Kocak, A.; Champeil, E. Quantitation of Amoxicillin in Urine by Nuclear Magnetic Resonance. Application to Five Cases. *J. Clin. Anal. Med.* **2016**, *7*, 65−69.
(73) http://moldb.wishartlab.com/system/documents/files/000/032/678/original/060519_P00_20_HW_1DP_256_Assigned20121204-3960-1sepfr4.png?1354670031. (Accessed January 14, 2021).

https://doi.org/10.1021/acsenvironau.2c00047
ACS Environ. Au 2023, 3, 47−55